

Slowing of axonal transport is a very early event in the toxicity of ALS-linked SOD1 mutants to motor neurons

Toni L. Williamson¹ and Don W. Cleveland^{1,2}

¹ Ludwig Institute for Cancer Research and ²Departments of Medicine and Neuroscience, University of California, San Diego, 9500 Gilman Drive, La Jolla, California 92093, USA

Correspondence should be addressed to D.W.C. (dccleveland@ucsd.edu)

Mutations in copper/zinc superoxide dismutase 1 (SOD1), primary causes of human amyotrophic lateral sclerosis (ALS), provoke motor neuron death through an unidentified toxic property. The known neurofilament-dependent slowing of axonal transport, combined with the prominent misaccumulation of neurofilaments in ALS, suggests that an important aspect of toxicity may arise from damage to transport. Here we verify this hypothesis for two SOD1 mutations linked to familial ALS. Reduced transport of selective cargoes of slow transport, especially tubulin, arises months before neurodegeneration. For one mutant, this represents the earliest detectable abnormality. Thus, damage to the cargoes or machinery of slow transport is an early feature of toxicity mediated by mutant SOD1.

ALS is a progressive neurodegenerative disease occurring in middle to late life and characterized by the loss of large motor neurons of the spinal cord, brain stem and motor cortex. Dysfunction and death of these motor neurons causes muscle weakness and atrophy leading to paralysis and death in 3–5 years¹. Approximately 10% of ALS cases are inherited in an autosomal dominant fashion. An estimated 15–20% of these familial ALS (FALS) patients have missense mutations in the gene encoding SOD1 (refs 2, 3), a metalloenzyme that catalyzes the formation of hydrogen peroxide through dismutation of superoxide anions⁴. SOD1 is thought to protect against cellular damage induced by oxygen radicals^{5,6}. The mechanism(s) through which mutations in SOD1 lead to late-onset motor neuron degeneration remains unidentified.

It was initially proposed that SOD1-linked FALS resulted from free radical damage due to decreased SOD1 activity^{3,7}. However, *in vitro*, different FALS-linked SOD1 mutants have different enzymatic activities, and at least some FALS mutations (for example, glycine changed to arginine at amino acid 37, or SOD1^{G37R}) retain full specific activity⁸. In addition, neither age of onset nor rapidity of progression correlate with SOD1 activity levels⁹, and SOD1 null mice live to adulthood and do not develop motor neuron disease¹⁰. Furthermore, transgenic mice expressing three different FALS mutants show progressive motor neuron disease despite elevated^{11,12} or unchanged^{13,14} levels of SOD1 activity, demonstrating that the FALS mutations in SOD1 act through the gain of a novel, cytotoxic property, rather than increased or decreased SOD1 activity. The mechanism of this cytotoxicity is currently unknown, although SOD1^{G85R} mice expressing high levels of wild-type SOD1 or deleted in the endogenous SOD1 alleles have shown that (at least for this mutant) toxicity is independent of SOD1 activity and the wild-type SOD1 polypeptide¹⁵.

Disruption of the neurofilament-L (NF-L) gene in SOD1 mutant mice to eliminate assembly and accumulation of axonal neurofilaments and/or subunits has shown that neurofilaments

are one determinant of the selectivity of motor neuron toxicity mediated by SOD1 mutants¹⁶. Moreover, aberrant perikaryal and axonal aggregates of neurofilaments are common hallmarks of both sporadic^{17,18} and SOD1-mediated^{19–21} ALS, and the large-caliber, neurofilament-rich axons are most at risk in mice¹⁴ and in human disease²². A plausible hypothesis for how neurofilaments may participate in motor neuron disease mechanism and selectivity arises from the known neurofilament-dependent slowing of slow axonal transport as neurofilaments accumulate to become the most abundant structural component of large-caliber axons²³. Because biosynthesis of macromolecules is almost completely restricted to the cell bodies, transport is especially crucial to these large-caliber axons. In humans, motor neurons can extend for more than a meter in length, yielding a cell volume about 5000 times that typical for an animal cell, almost all of which is in the axon²⁴. Overexpression of the largest human neurofilament subunit NF-H in mice results in perikaryal and axonal neurofilamentous accumulations accompanied by fine tremors, forelimb and muscle atrophy²⁵ and a slowing of slow axonal transport²⁶. When combined, these findings suggest that an important aspect of toxicity may arise from SOD1-mediated damage to the transport machinery or its cargoes. This in turn would promote motor axon degeneration through the simple mechanism of axonal strangulation.

Axonal transport has two components: transport of vesicles and mitochondria by kinesin and related proteins (fast transport) and movement of the major structural components of the neuron, many enzymes and other cytoplasmic proteins (slow transport). Slow transport can be divided into two components based on rate of movement: Sca (~0.5 mm/day), containing neurofilament proteins, tubulin and actin, and Scb (~1–2 mm/day), containing tubulin, actin and other cytoplasmic proteins²⁷. The mechanism of slow transport (and the motor(s) that power it) is unknown. To determine whether axonal transport defects may be

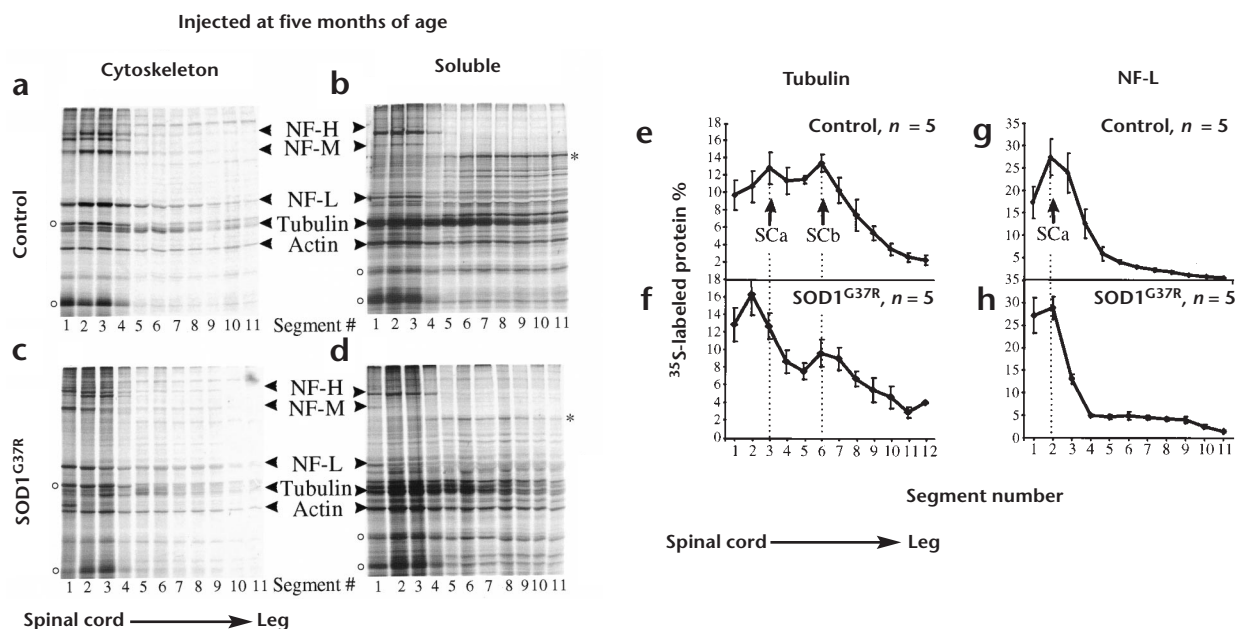


Fig. 1. Retardation of slow axonal transport before disease onset in SOD1^{G37R} mice. Fluorographs showing transport of [³⁵S]-labeled cytoskeletal (**a, c**) and soluble (**b, d**) proteins in sciatic nerve motor axons of control (**a, b**) and SOD1^{G37R} (**c, d**) mice. Each lane represents a consecutive 3-mm segment from L5 root and sciatic nerve of 6-month-old mouse killed 28 d after injection. Transport of tubulin (**e, f**) and NF-L (**g, h**) quantified by phosphorimaging shows that the transport of both proteins is slowed. Each value represents the average of five animals. Error bars show standard error. The asterisks (**b, d**) mark an unidentified component whose transport is reduced; open circles mark components whose transport remains unaffected.

involved in the pathogenesis of ALS, we examined the rate and composition of slow axonal transport in transgenic mice expressing the human SOD1^{G37R} and SOD1^{G85R} mutants. In both cases this slowing of slow axonal transport was evident at least six months before the onset of clinical signs, and in the case of SOD1^{G85R}, it occurred before any pathological changes were evident. No changes were detected in fast axonal transport, suggesting some selectivity towards slow transport. These results collectively demonstrate that changes in slow axonal transport are an early event in the toxicity arising from ALS-linked SOD1 mutants.

Results

EFFECTS ON TRANSPORT SIX MONTHS BEFORE DISEASE ONSET

To determine whether axonal transport is affected by the SOD1^{G37R} mutation, we examined the rate and composition of slow axonal transport in control ($n = 5$) and SOD1^{G37R} (line 106; $n = 5$) mice. [³⁵S]Methionine was injected into the spinal cord of five-month-old mice, six to seven months before onset of clinical symptoms. After 28 days, the L5 roots and sciatic nerve were removed intact, cut into 3-mm segments, homogenized and separated by centrifugation into soluble and cytoskeletal fractions. As expected, SDS-PAGE gels of labeled fractions from control mice clearly showed two waves of slow transport, SCa moving at ~0.25 mm per day and containing primarily neurofilament subunits, and SCb moving at ~0.75 mm per day and containing tubulin, actin and most cargoes of slow transport (Fig. 1a and b). Similar analyses of the labeled fractions from SOD1^{G37R} mice revealed both the faster (SCb) and slower (SCa) transport components (Fig. 1c and d). However, an obvious difference was that some proteins in both phases of transport moved significantly more slowly in the SOD1 mutant axons. In particular, transport of all three neurofilament subunits NF-L, NF-M and NF-H was markedly reduced. Phos-

phorimager quantitation of analyses from five mice of each genotype confirmed that neurofilament transport was slowed in SOD1^{G37R} mice by at least a factor of two (Fig. 1g and h).

Velocities of other cargoes normally moved in both waves of slow transport were also selectively retarded in the SOD1^{G37R} axons. This included a second major cytoskeletal component, tubulin; normally, a proportion of tubulin (both α and β) is moved in SCa and another portion in SCb (Fig. 1b). Whether tubulin moves as individual subunits, oligomers or polymers remains the subject of an unresolved debate^{28,29}. Our homogenization conditions cause disassembly of most axonal microtubules, so that ~80–90% of tubulin is found in the soluble fraction. In mice expressing the SOD1^{G37R} mutation, there was a marked shift in the proportion of tubulin in the slower phase as well as slowing in the movement velocity of this slower component (Fig. 1d and f). Transport of one unidentified SCb cargo (Fig. 1b and d, asterisk) was reduced in the mutant mice. These changes in transport reflect selective slowing of specific cargoes, because other components in both the cytoskeletal and soluble fractions (including the other major cytoskeletal component actin) were transported at approximately normal levels and rates. Thus, at least five to six months before clinical onset of disease, SOD1^{G37R} mutant-mediated damage affects transport of some, but not all, cargoes of slow transport.

TRANSPORT IS RETARDED EIGHT MONTHS BEFORE DEGENERATION

To determine how early the SOD1^{G37R} mutant affects slow axonal transport, we examined transport in mice injected with radiolabel at three months of age. In contrast to control mice injected at five months of age, in which tubulin is evenly distributed between SCa and SCb, more of the tubulin moves in the faster SCb fraction than in SCa in the younger control animals. How-

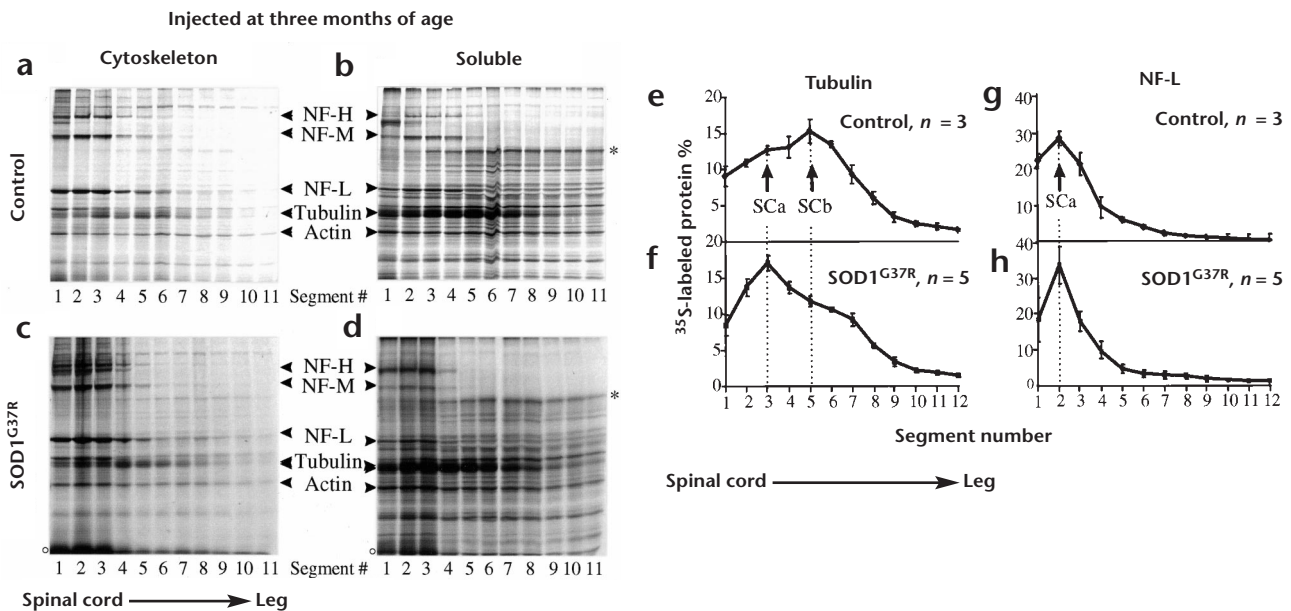


Fig. 2. Retardation of slow axonal transport seven months before disease onset in SOD1^{G37R} mice. Fluorographs showing transport of [³⁵S]-labeled cytoskeletal (a, c) and soluble (b, d) proteins in sciatic nerve motor axons of control (a, b) and SOD1^{G37R} (c, d) mice. Each lane represents a consecutive 3-mm segment from L5 root and sciatic nerve of 4-month-old mouse killed 28 d after injection. Transport of tubulin (e, f) and NF-L (g, h) quantified by phosphorimaging shows that the transport of tubulin is slowed. Each value represents the average of three (control) or five (transgenic) animals. Error bars show standard error. The asterisks (b, d) mark an unidentified component whose transport is reduced in Fig. 1 but remains unaffected at this earlier time point. The open circles mark an unidentified component whose transport is unaffected at both time points.

ever, even at this younger age, approximately seven months before clinical disease onset, tubulin transport was retarded in SOD1^{G37R} mice, with a large proportion shifted from SCb to SCa (Fig. 2d and f). This alteration in tubulin transport represents one of the initial transport defects, because at this early age no changes are detected in neurofilament transport or transport of other abundant axonal components, such as the unidentified component (Fig. 2b and d, asterisk) whose transport is clearly reduced at later time points (Fig. 1d).

Examination of the spinal cords of control and SOD1^{G37R} mice at four months of age, when tubulin transport is clearly slowed, revealed healthy-looking motor neuron perikarya (Fig. 3c and d). Despite the presence in axons of membrane-bounded vacuoles (Fig. 3d) that have been interpreted to arise from degenerating mitochondria¹², L5 ventral (Fig. 3a and b) and dorsal roots revealed no axonal degeneration in the SOD1^{G37R} line (106) mice at this age. Thus, SOD1^{G37R} causes selective disruption in axonal transport before the onset of axonal degeneration in these mice.

SLOW TRANSPORT IS DISRUPTED BEFORE DETECTABLE PATHOLOGY

To test whether selective defects in slow transport are a common feature of familial ALS-linked disease mediated by SOD1 mutants, we also examined mice that develop motor neuron disease from expressing SOD1^{G85R} (148). These mice have a similar age of onset to SOD1^{G37R} (106) mice (approximately 12 months of age), but the vacuolization found in SOD1^{G37R} mice does not occur at any stage of SOD1^{G85R}-mediated disease. Indeed, exhaustive examination of ventral roots (Fig. 3e and f) and spinal cords (Fig. 3g and h) of SOD1^{G85R} mice failed to detect any pathological changes, not only at six months of age, but even as late as eight to ten months of age¹⁴.

[³⁵S]Methionine was injected into the lumbar spinal cord of

five-month-old SOD1^{G85R} mice, and the animals were killed after 28 days, four to five months before pathology is detectable. Labeled proteins were quantified as before in 10–12 consecutive 3-mm segments extending from the spinal cord (L5 ventral root) to the sciatic nerve. This revealed that transport of tubulin is slower in mice expressing mutant SOD1^{G85R} (Fig. 4b, d, e and f). Not only did more of the tubulin move in the slower SCa wave than in control mice, but both SCa and SCb waves of tubulin transport moved at a reduced speed. This was especially so for the SCa portion of tubulin, whose apparent speed was reduced about 50% compared with wild-type mice. Once again this selective slowing was not unique to tubulin, with other SCb components including neurofilaments (Fig. 4g and h) and other less abundant components (Fig. 4b and d, asterisks) also slowed in mice expressing mutant SOD1, whereas other components, including actin, showed no marked change.

AXONAL SWELLINGS CONTAIN TUBULIN

The retardation of slow axonal transport, especially of tubulin, seen presymptomatically in both SOD1^{G37R} and SOD1^{G85R} mice might be expected to yield an increase in tubulin in perikarya and/or proximal axonal segments of spinal motor neurons compared with levels in control mice. To test this, we stained spinal cord sections from control, SOD1^{G37R} and SOD1^{G85R} mice with antibodies to β_{III} -tubulin, a neuron-specific isoform of β -tubulin³⁰ comprising at least 25% of neuronal β -tubulin³¹. Axonal swellings observed near the end stage of disease in both SOD1^{G37R} and SOD1^{G85R} mice showed intense reactivity for this neuronal tubulin (Fig. 5c–g), whereas no such aggregates were found in age-matched littermate controls. The abundance of tubulin immunoreactivity in prox-

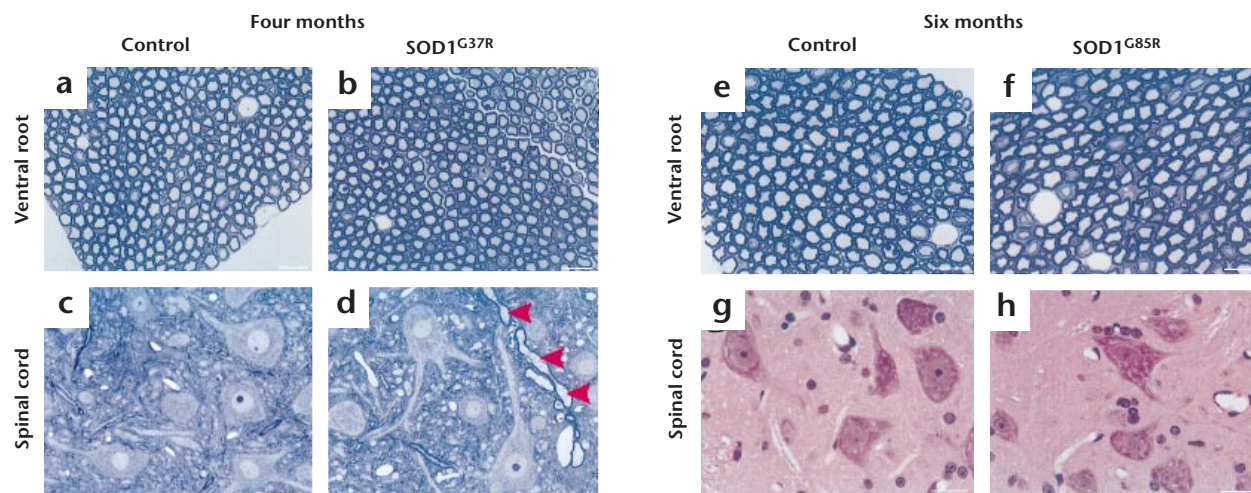


Fig. 3. Absence of motor neuron degeneration in $SOD1^{G37R}$ mice at four months of age and no detectable pathology in $SOD1^{G85R}$ mice at six months of age. Ventral root (**a, b**) and spinal cord motor neurons (**c, d**) from four-month-old control (**a, c**) and $SOD1^{G37R}$ (**b, d**) mice. Although degeneration of motor neurons was not yet evident, the proximal axons of ventral motor neurons already contained some vacuoles (arrows in **d**). Examination of ventral root (**e, f**) and spinal cord motor neurons (**g, h**) from six-month-old control (**e, g**) and $SOD1^{G85R}$ (**f, h**) mice reveals no evidence of any pathological changes. Scale bars, 25 μ m.

imal axon swellings in motor neurons of both $SOD1^{G37R}$ and $SOD1^{G85R}$ mice confirms that slow axonal transport is disrupted in these mice. In $SOD1^{G37R}$ mice, tubulin staining was excluded from the vacuoles but was found around and between vacuoles (Fig. 5e). In $SOD1^{G85R}$ mice, neuronal Lewy-body-like inclusions stained with antibodies to β_{III} -tubulin

(Fig. 5g), as did axonal swellings (Fig. 5f). Glial inclusions in $SOD1^{G85R}$ mice remain unstained (Fig. 5f).

Similar analyses using confocal immunofluorescence microscopy to examine tubulin distribution revealed that, compared with simultaneously processed images from wild-type animals (Fig. 6d), there was a reproducible, general reduction

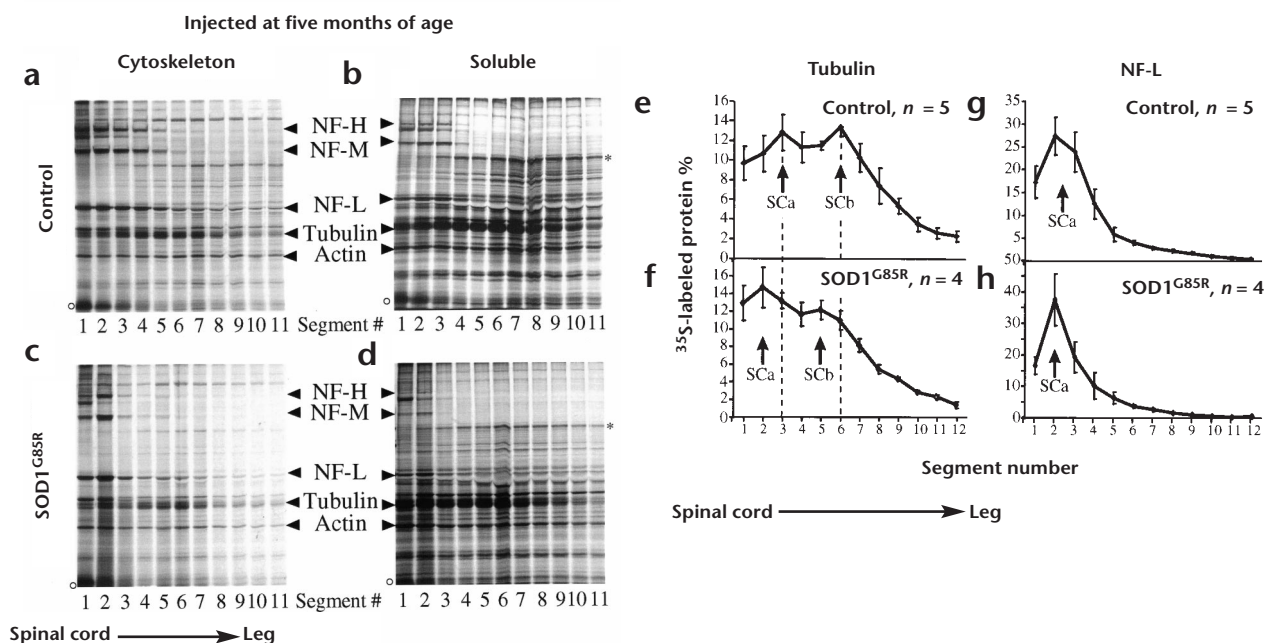


Fig. 4. Retardation of slow axonal transport before pathological changes in $SOD1^{G85R}$ mice. Fluorographs showing transport of [35 S]-labeled cytoskeletal (**a, c**) and soluble (**b, d**) proteins in sciatic nerve motor axons of control (**a, b**) and $SOD1^{G85R}$ (**c, d**) mice. Each lane represents a consecutive 3-mm segment from L5 root and sciatic nerve of 6-month-old mouse sacrificed 28 d after injection. Transport of tubulin (**e, f**) and NF-L (**g, h**) quantified by phosphorimaging shows that the transport of both proteins is slowed. Each value represents the average of four (transgenic) or five (control) animals. Error bars show standard error. The asterisks (**b, d**) mark an unidentified component whose transport is reduced; open circles mark components whose transport remains unaffected.

in staining of β_{III} -tubulin in axons in spinal cords from SOD1^{G37R} (Fig. 6e) and SOD1^{G85R} (Fig. 6f) mice, as well as relatively high levels in many cell bodies and proximal axons. Antibodies to neurofilament subunit NF-H showed its levels to be relatively unchanged (Fig. 6a–c). The absence of methionine in mature human SOD1 (and the small proportion of overall radiolabel incorporated into transported SOD1, ref. 32) precluded direct measurement of SOD1 mutant transport in the experiments reported above. However, to test whether slowing of tubulin transport was correlated with aggregates of SOD1 reported in both SOD1^{G85R} and SOD1^{G37R} mice^{14,15}, SOD1 and β_{III} -tubulin were localized in the same spinal cord sections. This revealed that the proximal accumulation of tubulin in motor neurons does not seem to require SOD1-containing axonal inclusions, because many neurons that are intensely immunoreactive for β_{III} -tubulin do not label with antibodies to SOD1 (Fig. 6g–i). Similarly, whereas some SOD1-immunoreactive inclusions were highly enriched for β_{III} -tubulin within or surrounding the SOD1 aggregate, especially in SOD1^{G85R} mice (Figs. 6h, i, k and l), many other SOD1 aggregates did not contain detectable β_{III} -tubulin (Fig. 6g and h), suggesting that the retardation of tubulin transport and SOD1 aggregation may arise independently.

FAST TRANSPORT IS NOT ALTERED BY SOD1 MUTATIONS

To determine whether fast axonal transport is also affected by mutant SOD1, we injected [³⁵S]methionine into the lumbar spinal cord of six-month-old control and SOD1^{G37R} mice. The mice were killed after three hours, and the speed of transport was assessed by measuring radiolabeled proteins along the L5 root and sciatic nerve. Unlike the slow transport protocol, for which radiolabeling provides a clear pulse-chase, the much higher rate of fast transport (and the correspondingly shorter time frame of the analysis) yields continuous labeling. Thus, a distinct transport peak is not visible, but the position of the front of the wave of fast transport denotes the rate of movement of its fastest components³³. At six months of age, when tubulin transport was clearly compromised in the mutant mice (Fig. 1), comparison of control and SOD1^{G37R} mice did not reveal any differences in the rates of fast transport (Fig. 7). Thus, most components of fast transport are unaffected by the SOD1 mutant, despite the presence of axonal vacuoles at this age in these mice.

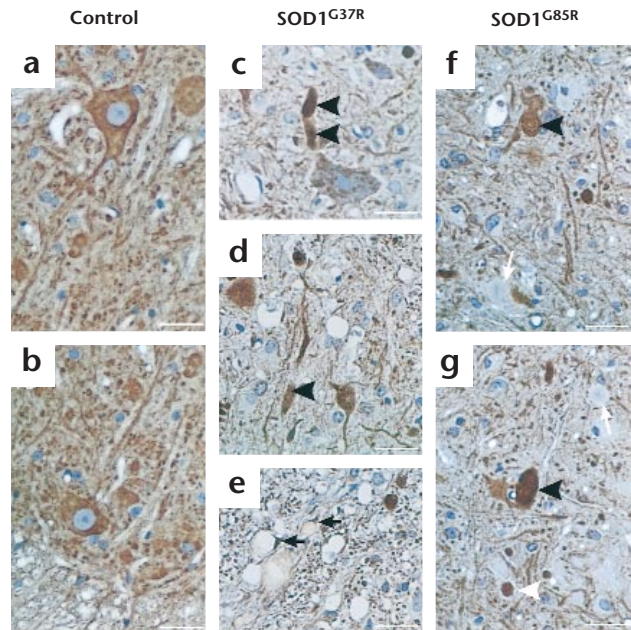


Fig. 5. Accumulation of β_{III} -tubulin in the proximal axons of SOD1 mutant mice. Motor neurons of mice expressing either SOD1^{G37R} (c–e) or SOD1^{G85R} (f, g) show inclusions highly immunoreactive for β_{III} -tubulin (black arrowheads), whereas no such aggregates are found in littermate controls (a, b). Tubulin staining is excluded from the vacuoles in SOD1^{G37R} mice (e). In SOD1^{G85R} mice nearing end stage of disease, axonal Lewy body-like inclusions stain with antibodies to β_{III} tubulin (f, white arrowheads), but glial inclusions remain unstained (f, g, white arrows). Scale bars, 25 μ m.

Discussion

We have shown that retardation of slow axonal transport is a very early event in mice expressing the FALS-linked SOD1^{G37R} and SOD1^{G85R} mutations. In SOD1^{G85R} mice, this is the earliest known abnormality, arising months before any pathological changes can be detected. Tubulin transport slows more dramatically at earlier stages, whereas the transport of neurofilaments and other cargoes yet to be identified is affected at later time

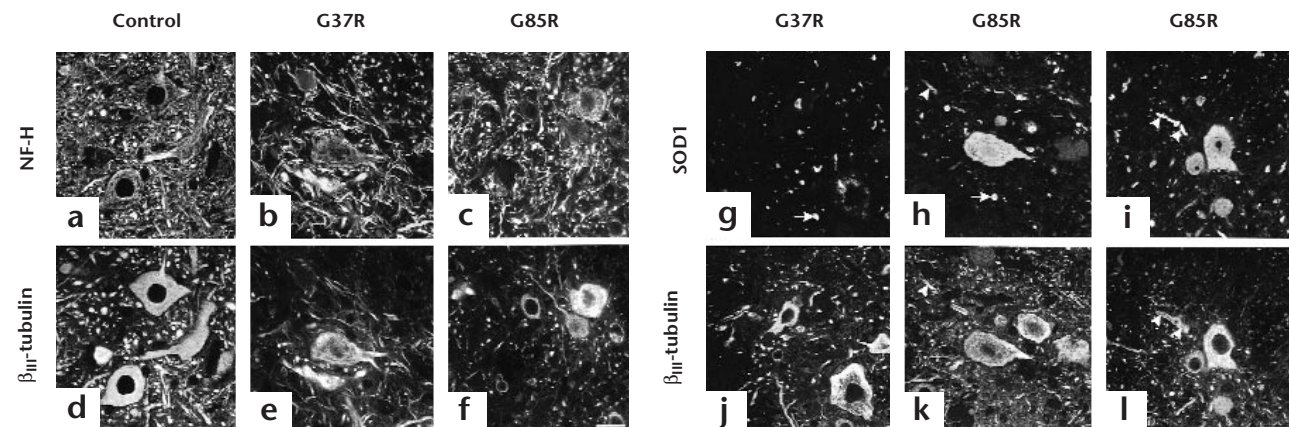
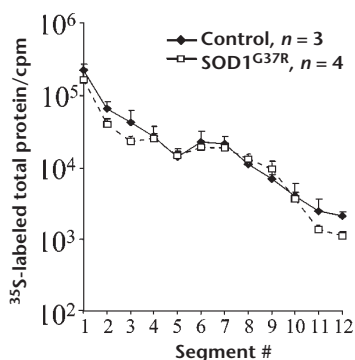


Fig. 6. Distinct localization of β_{III} -tubulin, NF-H and SOD1. Double immunostaining of spinal cord with antibodies to NF-H (a–c) or SOD1 (g–i) with β_{III} -tubulin (d–f, j–l) shows distinct but overlapping localization. Arrowheads point to SOD1-immunoreactive inclusions also highly enriched for β_{III} -tubulin within or surrounding the aggregate. Arrows point to SOD1 aggregates that did not stain for β_{III} -tubulin. Scale bar, 20 μ m.

Fig. 7. Fast axonal transport remains unaffected in SOD1^{G37R} mice. Fast transport of [³⁵S]-labeled proteins was measured in control (black line; *n* = 3) or SOD1^{G37R} (dashed line; *n* = 4) mice. Each point represents a consecutive three-mm segment from L5 root and sciatic nerve of six-month-old mouse killed three hours after injection. Error bars show standard error.



points, indicating a worsening of the defect, and presumably the underlying neuronal health and function with time. This is consistent with the slow accumulation of damage over a long period, ultimately culminating in late onset of disease in both mice and humans. Further support for a disruption in slow axonal transport early in disease comes from the obvious proximal axon swellings containing tubulin in both SOD1^{G37R} and SOD1^{G85R} mice. Collectively, these results show that axonal transport is an early target for SOD1-mediated damage arising from SOD1 mutants that cause markedly divergent pathologies.

The recent finding that a portion of SOD1 is transported in the SCb component of slow transport³² suggests that at least some of the damage to the motors and/or cargoes of slow transport may be mediated by the mutant SOD1 during its transport. Damage to tubulin and other proteins may simply result from their close proximity to the mutant SOD1 during transport. Further support for the involvement of axonal transport in SOD1 mutant-mediated ALS was provided by the observation that end-stage mice expressing the SOD1^{G93A} mutation also have slowed axonal transport³⁴, although it remains untested how early such changes occur. This evidence combines to support a model for SOD1 mutant toxicity mediated at least in part through chronic inhibition of the delivery of selected essential cargoes, most prominently tubulin. Over the long term, this results in slow depletion of such components from axons, ultimately culminating in axonal strangulation, leading to degeneration and death.

Consistent with the hypothesis that disruption of axonal transport would cause motor neuron dysfunction is the observation that transgenic mice overexpressing high levels of human NF-H develop a neuropathy characterized by muscle atrophy and a generalized tremor²⁵, and their slow axonal transport is compromised²⁶. In contrast, mice expressing similar levels of wild-type mouse NF-H (which differs in >160 amino-acid positions from human NF-H) show no phenotype and no general retardation of slow transport cargoes, despite a slowing of neurofilament transport³⁵. The increased vulnerability of large motor neurons to both the mutant SOD1 and to the overexpression of human NF-H might simply reflect the naturally high burden on the transport machinery within large motor neurons. This is further supported by the observation that only the largest neurofilament-rich motor axons are at risk in sporadic ALS²², in SOD1-mediated disease in mice¹⁴ and in mice expressing a neurofilament mutant that results in progressive motor neuron degeneration³⁶.

Further evidence linking one major cargo of slow transport to disease progression is the finding that complete elimination of neurofilaments, through disruption of the NF-L gene, delays onset of SOD1-mediated disease and extends life span by ~6 weeks¹⁶.

Because the rate of axonal transport decreases as the burden of axonal neurofilaments increases during development^{23,37,38} and regeneration³⁹, the delay in onset of clinical disease in NF-L null mice might result from an increase in the rate of axonal transport that compensates for slowing mediated by the SOD1 mutant. Similarly, increased synthesis of the large neurofilament subunit NF-H, which results in a loss of transport and/or assembly of neurofilaments in axons with motor neuron perikarya swollen with masses of disorganized filaments, can produce up to a six-month delay in onset of SOD1-mediated disease⁴⁰.

Whether the SOD1-mutant-dependent slowing of transport is a primary effect, due to direct damage to the transport machinery (and/or cargo) by the mutant enzymes, or a secondary event via an unidentified primary target, efficient axonal transport is essential for these very long neurons (particularly for the largest-caliber motor neurons that are naturally at risk in disease both in mice and in humans). Because binding of the catalytic copper is a common property of a series of ALS-linked mutants, including SOD1^{G37R} and SOD1^{G85R}⁴¹, it is possible that the mutants catalyze aberrant copper-mediated damage to specific motor(s) or cargoes of axonal transport by an as yet unidentified chemistry. Whatever the case, the present results provide evidence of a mechanism of SOD1 mutant action common to mutations that yield very different pathologies; long before the onset of clinical symptoms, compromised transport of selected cargoes contributes to motor neuron vulnerability through chronic reduction in these key axonal components.

Methods

CONSTRUCTION AND SCREENING OF TRANSGENIC MICE. The SOD1^{G37R} and SOD1^{G85R} mutations were engineered into the human SOD1 gene by PCR/oligonucleotide primer-directed mutagenesis¹². Mice carrying the SOD1 mutant transgene were identified by PCR screening of tail DNA using primers recognizing human and mouse SOD1 (5' CAG CAG TCA CAT TGC CCA AGG TCT CCA ACA T 3'), mouse SOD1 only (5' GTT ACA TAT AGG GGT TTA CTT CAT AA TCT G 3') and human SOD1 only (5' CCA AGA TGC TTA ACT CTT GTA ATC AAT GGC 3'). This reaction produces a ~800-bp mouse SOD1 PCR product and a ~600-bp human SOD1 PCR product.

MEASURING AXONAL TRANSPORT. Mice were anesthetized with Metafane (Mallinkrodt Veterinary Inc.) and maintained under anesthesia by continued inhalation of Metafane. Metabolic labeling of newly synthesized proteins was carried out by injecting 300 μ Ci of [³⁵S]methionine (Dupont NEN) into the ventral horn of the lumbar spinal cord. Twenty-eight days after injection, the L5 roots, dorsal root ganglia and approximately 3 cm of sciatic nerve were removed and cut into 3-mm segments. Each segment was homogenized on ice in a buffer containing 50 mM sodium phosphate, pH 7.15, 150 mM NaCl, 1 mM EDTA, 1% Triton X100, 0.9 M sucrose and 1 mM PMSF, then centrifuged at 12,000 g for 30 minutes at 4°C. Essentially all of the neurofilament proteins (NF-L, NF-M and NF-H), along with cold insoluble tubulin and actin, were recovered in the pellet fraction. The entire pellet was resolubilized in 2% SDS-containing gel sample buffer. Pellets and supernatants were run on 7% SDS-PAGE gels. Gels were stained with Coomassie blue, destained and the proteins visualized by fluorography (Enhance, Dupont NEN). Bands were quantified using a Molecular Dynamics Phosphorimager. Approximately 80–90% of the tubulin was found in the soluble fraction under the lysis conditions used above. The results shown are for transport of this soluble tubulin, however, tubulin in the insoluble fraction and total tubulin were also analyzed, with the same results.

For fast axonal transport experiments, 100 μ Ci of [³⁵S]methionine was injected as above and the mouse killed after 3 hours. The nerves were dissected (as above) and homogenized in a buffer containing 25 mM sodium phosphate, pH 7.2, 5 mM EDTA and 1% SDS. Proteins from each segment of nerve were precipitated with trichloroacetic acid (20%

final), immobilized onto a glass filter (Whatman GC/K), washed and counted using a scintillation counter (Beckman).

HISTOLOGICAL ANALYSIS. Mice anesthetized with an intraperitoneal injection of 0.02 ml/g avertin (tribromoethanol and tertamyl alcohol) were killed by transcardiac perfusion with 0.1 M sodium phosphate, followed by 4% formaldehyde, 2.5% glutaraldehyde in 0.1 M sodium phosphate, pH 7.6. Tissues were incubated in 2% osmium tetroxide in 0.05 M cacodylate for 3.5 hours, washed, dehydrated and embedded in Epon-Araldite resin (Ernest F. Fullam, Inc.). Sections (0.75 μ m) were stained with toluidine blue and examined by light microscopy. For immunohistochemistry, mice were perfused with 4% formaldehyde in 0.1 M sodium phosphate, pH 7.6. Spinal cords were removed, post-fixed in the same solution and embedded in paraffin. Sections (10 μ m) were deparaffinized, rehydrated, then quenched in methanol and 0.3% hydrogen peroxide for 30 minutes. Sections were rinsed in PBS and incubated overnight in primary antibody recognizing the neuron specific β_{III} tubulin³⁰ (supplied by A. Frankfurter). Sections were incubated for 30 minutes in a biotinylated secondary antibody, rinsed with PBS, then incubated in a peroxidase-conjugated antibody (Vectastain ABC kit, Vector Laboratories). The immunoreactivity was visualized with diaminobenzidine, and sections were counter-stained with hematoxylin. For immunofluorescence, 40- μ m vibratome sections were incubated overnight with primary antibodies recognizing neuron-specific β_{III} tubulin³⁰, the carboxyl terminus of NF-H⁴² or human-mouse SOD1⁴³, rinsed with PBS, then incubated with texas red and fluorescein-labeled secondary antibodies (Capell).

Acknowledgements

We acknowledge Karen L. Anderson, Janet S. Folmer and Scott D. Anderson for technical assistance. This work was supported by grant NS 27036 from the NIH and a grant from the Muscular Dystrophy Association to D.W.C. T.L.W. was supported, in part, by a postdoctoral fellowship from the Muscular Dystrophy Association. Salary support for D.W.C. is provided by the Ludwig Institute for Cancer Research.

RECEIVED 20 OCTOBER; ACCEPTED 16 NOVEMBER 1998

1. Williams, D. B. & Windebank, A. J. *Peripheral Neuropathy* (eds Dyck, P. J., Thomas, P. K., Griffin, J. W., Low, P. A. & Poduslo, J. E.) 1028–1050 (W.B. Saunders, Philadelphia, 1993).
2. Rosen, D. R. *et al.* Mutations in Cu/Zn superoxide dismutase gene are associated with familial amyotrophic lateral sclerosis. *Nature* **362**, 59–62 (1993).
3. Deng, H.-X. *et al.* Amyotrophic lateral sclerosis and structural defects in Cu, Zn superoxide dismutase. *Science* **261**, 1047–1051 (1993).
4. Fridovich, I. Superoxide radical and superoxide dismutases. *Annu. Rev. Biochem.* **64**, 97–112 (1995).
5. Halliwell, B. Free radicals, antioxidants, and human disease: curiosity, cause, or consequence? *Lancet* **344**, 721–724 (1994).
6. Yu, B. P. Cellular defenses against damage from reactive oxygen species. *Physiol. Rev.* **74**, 139–162 (1994).
7. Bowling, A. C., Schulz, J. B., Brown, R. H. Jr & Beal, M. F. Superoxide dismutase activity, oxidative damage, and mitochondrial energy metabolism in familial and sporadic amyotrophic lateral sclerosis. *J. Neurochem.* **61**, 2322–2325 (1993).
8. Borchelt, D. R. *et al.* Superoxide dismutase 1 with mutations linked to familial amyotrophic lateral sclerosis possesses significant activity. *Proc. Natl. Acad. Sci. USA* **91**, 8292–8296 (1994).
9. Cleveland, D. W., Laing, N., Hulse, P. V. & Brown, R. H. Toxic mutants in Charcot's sclerosis. *Nature* **378**, 342–343 (1995).
10. Reaume, A. B. *et al.* Motor neurons in Cu/Zn superoxide dismutase-deficient mice develop normally but exhibit enhanced cell death after axonal injury. *Nat. Genet.* **13**, 43–47 (1996).
11. Gurney, M. E. *et al.* Motor neuron degeneration in mice that express a human Cu,Zn superoxide dismutase mutation. *Science* **264**, 1772–1775 (1994).
12. Wong, P. C. *et al.* An adverse property of a familial ALS-linked SOD1 mutation causes motor neuron disease characterized by vacuolar degeneration of mitochondria. *Neuron* **14**, 1105–1116 (1995).
13. Ripps, M. E., Huntley, G. W., Hof, P. R., Morrison, J. H. & Gordon, J. W. Transgenic mice expressing an altered murine superoxide dismutase gene provide an animal model of amyotrophic lateral sclerosis. *Proc. Natl. Acad. Sci. USA* **92**, 689–693 (1995).
14. Bruijn, L. I. *et al.* ALS-linked SOD1 mutant G85R mediates damage to astrocytes and promotes rapidly progressive disease with SOD1-containing inclusions. *Neuron* **18**, 327–338 (1997).
15. Bruijn, L. I. *et al.* Mutant-SOD1 mediated Amyotrophic Lateral Sclerosis disease onset, progression and pathology is independent of wild-type

- protein. *Science* **281**, 1851–1854 (1998).
16. Williamson, T. L. *et al.* Absence of neurofilaments reduces the selective vulnerability of motor neurons and slows disease caused by a familial ALS-linked SOD1 mutant. *Proc. Natl. Acad. Sci. USA* **95**, 9631–9636 (1998).
17. Banker, B.Q. *Myology* (eds Engel, A. G. & Banker, B. Q.) 2031–2066 (McGraw-Hill, New York, 1986).
18. Hirano, A., Donnenfeld, H., Sasaki, S. & Nakano, I. Fine structural observations of neurofilamentous changes in amyotrophic lateral sclerosis. *J. Neuropathol. Exp. Neurol.* **43**, 461–470 (1984).
19. Hirano, A. *et al.* Fine structural study of neurofibrillary changes in a family with amyotrophic lateral sclerosis. *J. Neuropathol. Exp. Neurol.* **43**, 471–480 (1984).
20. Shibata, N. *et al.* Intense superoxide dismutase-1 immunoreactivity in intracytoplasmic hyaline inclusions of familial amyotrophic lateral sclerosis with posterior column involvement. *J. Neuropathol. Exp. Neurol.* **55**, 481–490 (1996).
21. Rouleau, G. A. *et al.* SOD1 mutation is associated with accumulation of neurofilaments in Amyotrophic Lateral Sclerosis. *Ann. Neurol.* **39**, 128–131 (1996).
22. Kawamura, Y. *et al.* Morphometric comparison of the vulnerability of peripheral motor and sensory neurons in amyotrophic lateral sclerosis. *J. Neuropathol. Exp. Neurol.* **40**, 667–675 (1981).
23. Willard, M. & Simon, C. Modulations of neurofilament axonal transport during the development of rabbit retinal ganglion cells. *Cell* **35**, 551–559 (1983).
24. Williamson, T. L. *et al.* Neurofilaments, radial growth of axons, and mechanisms of motor neuron disease. *Cold Spring Harb. Symp. Quant. Biol.* **61**, 709–723 (1996).
25. Côté, F., Collard, J. F. & Julien, J. P. Progressive neuronopathy in transgenic mice expressing the human neurofilament heavy gene: a mouse model of amyotrophic lateral sclerosis. *Cell* **73**, 35–46 (1993).
26. Collard, J. F., Côté, F. & Julien, J. P. Defective axonal transport in a transgenic mouse model of amyotrophic lateral sclerosis. *Nature* **375**, 61–64 (1995).
27. Hoffman, P. N. & Lasek, R. J. The slow component of axonal transport. Identification of major structural polypeptides of the axon and their generality among mammalian neurons. *J. Cell Biol.* **66**, 351–366 (1975).
28. Hirokawa, N. The mechanisms of fast and slow transport in neurons: identification and characterization of the new kinesin superfamily motors. *Curr. Opin. Neurobiol.* **7**, 605–614 (1997).
29. Baas, P. W. Microtubules and axonal growth. *Curr. Opin. Cell Biol.* **9**, 29–36 (1997).
30. Lee, M. K., Rebhun, L. I. & Frankfurter, A. Posttranslational modification of class III beta-tubulin. *Proc. Natl. Acad. Sci. USA* **87**, 7195–7199 (1990).
31. Lopata, M. A. & Cleveland, D. W. In vivo microtubules are copolymers of available beta-tubulin isotypes: localization of each of six vertebrate beta-tubulin isotypes using polyclonal antibodies elicited by synthetic peptide antigens. *J. Cell Biol.* **105**, 1707–1720 (1987).
32. Borchelt, D. R. *et al.* Axonal transport of mutant superoxide dismutase 1 and focal axonal abnormalities in the proximal axons of transgenic mice. *Neurobiol. Dis.* **5**, 27–35 (1998).
33. Mitsumoto, H., Kurahashi, K., Jacob, J. M. & McQuarrie, I. G. Retardation of fast axonal transport in wobbler mice. *Muscle Nerve* **16**, 542–547 (1993).
34. Zhang, B., Tu, P., Abtahian, F., Trojanowski, J. Q. & Lee, V. M. Neurofilaments and orthograde transport are reduced in ventral root axons of transgenic mice that express human SOD1 with a G93A mutation. *J. Cell Biol.* **139**, 1307–1315 (1997).
35. Marszalek, J. R. *et al.* Neurofilament subunit NF-H modulates axonal diameter by selectively slowing neurofilament transport. *J. Cell Biol.* **135**, 711–724 (1996).
36. Lee, M. K., Marszalek, J. & Cleveland, D. W. Expression of a mutant neurofilament subunit causes massive, selective motor neuron death and ALS-like motor neuron disease. *Neuron* **13**, 975–988 (1994).
37. Hoffman, P. N., Lasek, R. J., Griffin, J. W. & Price, D. L. Slowing of the axonal transport of neurofilament proteins during development. *J. Neurosci.* **3**, 1694–1700 (1983).
38. Hoffman, P. N., Griffin, J. W., Gold, B. G. & Price, D. L. Slowing of neurofilament transport and the radial growth of developing nerve fibers. *J. Neurosci.* **5**, 2920–2929 (1985).
39. Hoffman, P. N., Thompson, G. W., Griffin, J. W. & Price, D. L. Changes in neurofilament transport coincide temporally with alterations in the caliber of axons in regenerating motor fibers. *J. Cell Biol.* **101**, 1332–1340 (1985).
40. Couillard-Depres, S. *et al.* Protective effect of neurofilament over-expression in motor neuron disease induced by mutant superoxide dismutase. *Proc. Natl. Acad. Sci. USA* **95**, 9626–9630 (1998).
41. Corson, L. B., Strain, J. J., Culotta, V. C. & Cleveland, D. W. Chaperone-facilitated copper binding is a property common to several classes of familial amyotrophic lateral sclerosis-linked superoxide dismutase mutants. *Proc. Natl. Acad. Sci. USA* **95**, 6361–6366 (1998).
42. Xu, Z., Cork, L. C., Griffin, J. W. & Cleveland, D. W. Increased expression of neurofilament subunit NF-L produces morphological alterations that resemble the pathology of human motor neuron disease. *Cell* **73**, 23–33 (1993).
43. Pardo, C. A. *et al.* Superoxide dismutase is an abundant component in cell bodies, dendrites, and axons of motor neurons and in a subset of other neurons. *Proc. Natl. Acad. Sci. USA* **92**, 954–958 (1995).